

## Model for the x-ray photoelectron distributions of $d$ -band perovskites

T. Wolfram\*

Argonne National Laboratory, Argonne, Illinois 60439

Ş. Ellialtıođlu†

Department of Physics, University of Missouri-Columbia, Columbia, Missouri 65201

(Received 28 October 1977; revised manuscript received 2 February 1978)

An analytical model for the photoelectron energy distribution function for cubic  $d$ -band perovskites is presented, which includes the effects of differences in the  $p$  and  $d$  electron cross sections and plasmon excitation due to many-body interactions. The model provides a simple method for interpreting x-ray-photoemission data in terms of band structure. Excellent agreement between experiment and theory is demonstrated for both SrTiO<sub>3</sub> and Na<sub>0.8</sub>WO<sub>3</sub>.

Recently a number of XPS (x-ray photoelectron spectroscopy) investigations have been reported for the transition-metal oxides having the cubic perovskite structure. These studies include SrTiO<sub>3</sub>,<sup>1</sup> ReO<sub>3</sub>,<sup>2</sup> H<sub>x</sub>WO<sub>3</sub>,<sup>3</sup> and Na<sub>x</sub>WO<sub>3</sub>.<sup>3,4</sup> Both XPS and UPS (ultraviolet photoelectron spectroscopy) spectra have been reported for SrTiO<sub>3</sub>.<sup>1,5,6</sup>

A central objective of these studies is to relate the photoelectron spectra to the electronic structure of the perovskites. However, direct comparison of XPS spectra with the energy bands or the total filled DOS (density of states) is unsatisfactory because the photoelectron cross section  $\sigma(p)$  for electrons in oxygen  $p$  orbitals is substantially smaller than  $\sigma(d)$  for the transition-metal  $d$ -orbital electrons. In addition, for metallic perovskites such as the alkali tungsten bronzes or ReO<sub>3</sub>, XPS valence-band spectra are significantly modified by very strong many-body effects including plasmon excitation due to hole-electron interactions.<sup>4,7</sup>

In order to interpret XPS data for the perovskites it is necessary to have the PDOS (partial density of state) functions for the  $p$  and  $d$  electrons separately and to include the many-body plasmon effect. The EDC (energy distribution curve) can then be analyzed in terms of a weighted sum of PDOS functions, where  $\sigma(p)$  and  $\sigma(d)$  are the weighting factors. Unfortunately, except for a recent calculation by Kopp *et al.*,<sup>8</sup> the PDOS functions for perovskites are not known.

In this article we present simple analytical expressions for the PDOS functions for an arbitrary cubic  $d$ -band perovskite. Using the results we then obtained a formula for the EDC which includes cross-section and plasmon effects. Excellent agreement between the theoretical EDC's and XPS spectra of SrTiO<sub>3</sub> and Na<sub>0.8</sub>WO<sub>3</sub> is demonstrated. As a product of these analyses we find that  $\sigma(p)/\sigma(d) = \frac{1}{3}$  for SrTiO<sub>3</sub> and  $\frac{1}{12}$  for Na<sub>0.8</sub>WO<sub>3</sub> for 1486.6-eV photons. Furthermore we find that the probability of plasmon excitation due to

shallow hole relaxation is 0.2, which is the same for *core-hole* relaxation<sup>4</sup> in Na<sub>0.8</sub>WO<sub>3</sub>.

In a previous paper<sup>9</sup> we presented analytical formulas for the total DOS of the perovskites and demonstrated excellent agreement with energy-band calculations for SrTiO<sub>3</sub>, KTaO<sub>3</sub>, ReO<sub>3</sub>,<sup>10</sup> and NaWO<sub>3</sub>.<sup>8</sup> In this article we present analytical results for the PDOS functions and the EDC of a perovskite. The linear combination of atomic orbitals (LCAO) model from which we derive these results has been described in detail elsewhere<sup>9,11</sup> and need not be reviewed here.

The results for the PDOS functions are

$$\begin{aligned} \rho_p(E) = & 3 \frac{\frac{1}{2}(E - E_{\pi^*})}{(pd\pi)^2} \rho_{\pi}(E) + \frac{(E - E_{\sigma^*})}{(pd\sigma)^2} \rho_{\sigma}(E) \\ & + 3 \left( \frac{\lambda_{\pi^{\circ}}}{\pi} \right)^{1/2} \exp[-\lambda_{\pi^{\circ}}(E - E_{\pi^{\circ}})^2] \\ & + \left( \frac{\lambda_{\sigma^{\circ}}}{\pi} \right)^{1/2} \exp[-\lambda_{\sigma^{\circ}}(E - E_{\sigma^{\circ}})^2], \end{aligned} \quad (1)$$

$$\rho_d(E) = 3 \frac{\frac{1}{2}(E - E_{\pi})}{(pd\pi)^2} \rho_{\pi}(E) + \frac{(E - E_{\sigma})}{(pd\sigma)^2} \rho_{\sigma}(E), \quad (2)$$

where  $\rho_p$  and  $\rho_d$  are the  $p$ - and  $d$ -orbital PDOS functions, respectively. The band-edge energies  $E_{\pi}$ ,  $E_{\pi^*}$ ,  $E_{\sigma}$ ,  $E_{\sigma^*}$ ,  $E_{\pi^{\circ}}$ , and  $E_{\sigma^{\circ}}$ , the universal density functions  $\rho_{\pi}(E)$  and  $\rho_{\sigma}(E)$ , as well as the LCAO parameters  $pd\pi$  and  $pd\sigma$  are defined in our previous paper.<sup>9</sup> The parameters  $\lambda_{\pi^{\circ}}$  and  $\lambda_{\sigma^{\circ}}$  determined the widths of the oxygen nonbonding bands and theoretically these are  $\lambda_{\pi^{\circ}} \approx \ln 2 / (pp\sigma - pp\pi)^2$  and  $\lambda_{\sigma^{\circ}} = \frac{1}{4}\lambda_{\pi^{\circ}}$ , where  $pp\sigma$  and  $pp\pi$  are the LCAO oxygen-oxygen interactions matrix elements.<sup>11</sup>

The photoelectron EDC  $N(E)$  is the rate of emission of electrons from initial states of energy  $E$  into final states of energy  $E + h\nu$ , where  $h\nu$  is the incident photon energy. For XPS, assuming a constant final-state density of states and no dif-

ferential relaxation,  $N(E)$  is approximately

$$N(E) \approx A[\rho_d(E) + \{\sigma(p)/\sigma(d)\}\rho_p(E)]f(E), \quad (3)$$

where  $f(E)$  is the Fermi distribution function and  $A$  is a scaling constant.

For metallic perovskites, hole relaxation has a very high probability of creating a plasmon of energy  $E_p$ . When this occurs an electron emitted from an initial state of energy  $E$  will appear to have originated from an initial state of energy  $E - E_p$ . This effect can be included by using the "apparent" distribution function,  $N'(E)$  defined as

$$N'(E) = (1 - \beta)N(E) + \beta(1/\Gamma\sqrt{\pi}) \times \int_{-\infty}^{\infty} dE' \exp\left[-\left(\frac{E - E'}{\Gamma}\right)^2\right] N(E' + E_p), \quad (4)$$

where  $\beta$  is the probability of plasmon creation and  $2\sqrt{\ln 2} \Gamma$  is the FWHM (full width at half maximum) of the lifetime-broadened plasmon band.

To compare theory directly with experiments  $N'(E)$  must be broadened to account for the experimental resolution. The resulting distribution,  $\langle N'(E) \rangle$ , is given by

$$\langle N'(E) \rangle = \int_{-\infty}^{\infty} dE' \exp\left[-\left(\frac{E - E'}{R}\right)^2\right] N'(E'), \quad (5)$$

where  $2\sqrt{\ln 2} R$  is the FWHM experimental resolution.

Equations (1)–(5) provide a prescription for calculating the XPS spectrum of any cubic perovskite in terms of electronic structure and width parameters. Conversely, the model can be used

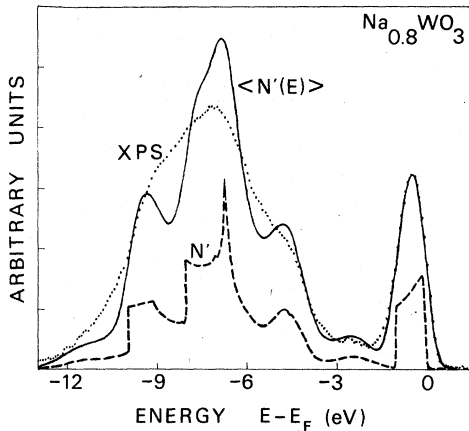


FIG. 1. Comparison of the theoretical EDC (this work) with the XPS data (dots) of Ref. 4 for  $\text{Na}_{0.8}\text{WO}_3$ . The dashed curve is the  $N'(E)$  from Eq. (4) with parameters (in eV);  $E_{\sigma^*} = 1.8$ ,  $E_{\pi^*} = -1.05$ ,  $E_{\tau_0} = -4.6$ ,  $E_{\tau} = -4.6$ ,  $E_{\sigma_0} = -5.0$ ,  $E_{\sigma} = -7.0$   $pd\pi = 1.73$ ,  $pd\sigma = -2.4$ ,  $pp\pi = -0.20$ ,  $pp\sigma = 0.46$ ,  $E_p = 2.0$ ,  $\Gamma = 0.76$ , and  $\beta = 0.2$ ,  $\sigma(p)/\sigma(d) = \frac{1}{12}$ . The solid curve is  $\langle N'(E) \rangle$  from Eq. (5) with  $R = 0.42$  eV.

to infer the electronic structure by fitting the XPS spectrum.

To demonstrate the utility of the model we have applied it to the analysis of an insulating ( $\text{SrTiO}_3$ ) and a metallic ( $\text{Na}_{0.8}\text{WO}_3$ ) perovskite XPS spectrum.

The results for  $\text{Na}_{0.8}\text{WO}_3$  are shown in Fig. 1. The dashed curve is  $N'(E)$  [Eq. (4)], the solid curve is  $\langle N'(E) \rangle$  [Eq. (5)] and the dotted curve is the XPS data of Chazalviel *et al.*<sup>4</sup> As a result of the analysis, the spectrum may be interpreted as follows: the peak near the Fermi level  $E_F$  is from the electrons of the partially filled  $\pi^*$  conduction band; the small peak in the band-gap region ( $\sim -1$  to  $-3$  eV) is due to conduction electrons shifted down in energy by  $E_p = 2.0$  eV due to plasmon creation associated with hole relaxation; the peak (shoulder) near  $-4.5$  eV is due to emission from the non-bonding bands ( $\pi^0$  and  $\sigma^0$ ); the large central peak arises from the logarithmic singularity in the  $\pi$ -valence-band DOS; the lowest peak, near  $-9$  eV, is produced by the jump discontinuity in the DOS at the bottom of the  $\sigma$  band; and the tail from  $-10$  to  $-12$  eV is due to  $\sigma$ -band electrons shifted down by  $E_p$ .

In calculating  $\langle N'(E) \rangle$ , the LCAO parameters  $pd\pi$ ,  $pd\sigma$ ,  $pp\pi$ , and  $pp\sigma$  were determined from available energy-band calculations.<sup>8</sup>  $E_{\tau}$  and  $E_{\tau^*}$  are then *uniquely* determined by the requirement that 0.8 electrons are in the  $\pi^*$  band. The values  $E_p = 2$  eV,  $\Gamma = 0.76$  eV,  $\beta = 0.2$ , and  $R = 0.42$  eV are those determined by Chazalviel *et al.*<sup>4</sup> from analysis of *core-level* emission. The shoulder in the XPS data at about  $-10$  eV fixes  $E_{\sigma}$  and the shoulder near  $-4$  eV locates  $E_{\pi^0}$  and  $E_{\sigma^0}$  within about  $\pm \frac{1}{2}$  eV. Thus the only truly adjustable parameter was  $\sigma(p)/\sigma(d)$ . It was determined by requiring that the ratio of the conduction- to valence-band emission areas be equal to that observed experimentally,<sup>4</sup> namely, 0.21. This gives  $\sigma(p)/\sigma(d) = \frac{1}{12}$ , which is somewhat larger than that found by Wertheim *et al.*<sup>2</sup> for  $\text{ReO}_3$ .

The agreement between  $\langle N'(E) \rangle$  and the XPS data is remarkably good; the bandwidths, and locations of all of the characteristic structure agrees with experiment including the plasmon effects. The  $\langle N'(E) \rangle$  in the region 0 to  $-3$  eV, due to conduction electrons and the plasmon effect, fits the data nearly exactly and this region is essentially independent of the varied parameters. The theory agrees well with the valence-band emission as well, however, there does appear to be broadening of the data relative to the predicted emission.

As a second application of the model we have analyzed the XPS data of Battye, Hochst, and Goldman<sup>1</sup> for  $\text{SrTiO}_3$ . The results are shown in Fig. 2(a)–2(c). In Fig. 2(b) the data (dots) and

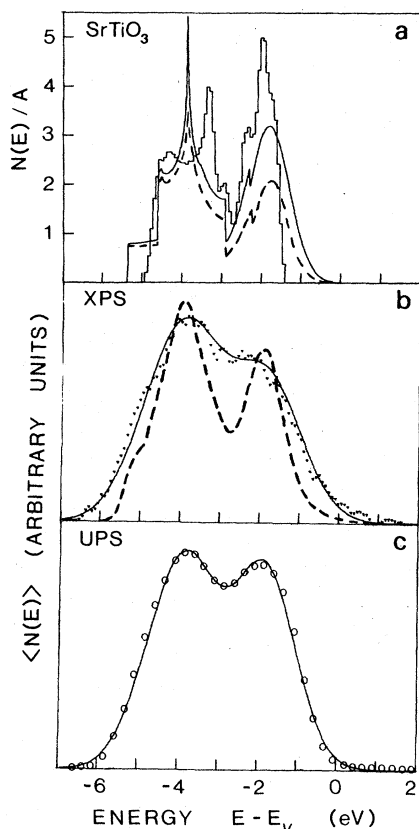


FIG. 2. Comparison of the theoretical EDC with the XPS and UPS data for SrTiO<sub>3</sub>. (a) Total DOS histogram of Mattheiss, Ref. 10, is compared with  $N(E)/A$  from Eq. (3) with  $\sigma(p)/\sigma(d)=1$  in units of states/spin cell eV with parameters (in eV):  $E_{\pi^*} = 5.0$ ,  $E_{\pi^*} = 3.25$ ,  $E_{\sigma^0} = 1.6$ ,  $E_{\pi^0} = -1.9$ ,  $E_{\sigma^0} = -2.3$ ,  $E_{\pi^0} = -2.9$ ,  $pd\pi = 1.3$ ,  $pd\sigma = -2.3$ ,  $pp\pi = -0.107$ ,  $pp\sigma = 0.426$  (solid line). The dashed curve is the same as solid curve except for  $\sigma(p)/\sigma(d) = \frac{1}{3}$ . (b) The dashed curve is  $\langle N(E) \rangle$  from Eq. (5) with  $\beta = 0$ ,  $\sigma(p)/\sigma(d) = \frac{1}{3}$ , and  $R = 0.33$  eV and the full curve with  $R = 0.8$  eV is compared with the XPS data of Ref. 1 (in dots). (c) Full curve is the  $\langle N(E) \rangle$  from Eq. (5) with  $\beta = 0$ ,  $\sigma(p)/\sigma(d) = 1$  and  $R = 0.8$  eV compared with the UPS data of Ref. 5 (in circles).

$\langle N'(E) \rangle$  for two different experimental resolutions (dashed and solid curves) are shown. The dashed  $\langle N'(E) \rangle$  curve is for the quoted instrumental resolution of 0.55 eV ( $R = 0.33$  eV) and the solid curve is for an effective resolution of 1.35 eV ( $R = 0.8$  eV). The agreement between experiment and theory for the latter resolution is remarkably good.

The parameters for SrTiO<sub>3</sub> were determined in a manner similar to that used for Na<sub>0.8</sub>WO<sub>3</sub>. The parameters  $pd\sigma$ ,  $pd\pi$ ,  $pp\sigma$ , and  $pp\pi$  were determined from energy-band calculations<sup>10,11</sup> and  $\beta = 0$  (no plasmon effect). The known band gap<sup>12</sup> gives  $E_{\pi^*} - E_{\pi^0} = 3.25$  eV. The band edges  $E_{\pi^*}$ ,  $E_{\sigma^*}$ ,  $E_{\sigma^0}$ ,  $E_{\pi^0}$ , and  $E_{\sigma^0}$  were chosen to fit the locations of the two peaks in the data. The ratio  $\sigma(p)/\sigma(d)$  was varied to fit the relative peak heights and was found to be  $\frac{1}{3}$ .

Figure 2(a) shows the function  $N(E)$  for SrTiO<sub>3</sub> for  $\sigma(p)/\sigma(d) = 1$  (solid curve) and for  $\sigma(p)/\sigma(d) = \frac{1}{3}$  (dashed curve) and the DOS histogram derived by Mattheiss.<sup>10</sup> Since  $N(E)$  for  $\sigma(p)/\sigma(d) = 1$  is the DOS it may be compared directly with the histogram. The major differences are that the  $\pi$ -band peak of  $N(E)$  is shifted about  $\frac{1}{2}$  eV to lower energy and the total width of the nonbonding bands is about 30% wider than for the histogram. The individual nonbonding bands ( $\pi^0$  and  $\sigma^0$ ) have widths that are comparable to those represented by the histogram but they are more widely separated resulting in the appearance of a single broader band.

As a further use of the model the UPS spectrum of Henrich *et al.*<sup>5</sup> was compared with  $\langle N'(E) \rangle$ . Figure 2(c) shows  $\langle N'(E) \rangle$  with  $\sigma(p)/\sigma(d) = 1$  (solid curve) compared with the UPS data (open circles). All of the parameters are the same as used for  $\langle N'(E) \rangle$  in Fig. 2(b) [except  $\sigma(p)/\sigma(d) = 1$ ]. The agreement between the UPS data and theory is essentially exact. This analysis suggests that the UPS spectrum (at 21.2 eV) closely resembles the total DOS while for XPS (at 1486 eV)  $\sigma(p)$  is about  $\frac{1}{3}$  of  $\sigma(d)$ .

In conclusion, we believe that the model presented here will be of great value for the analysis and interpretation of XPS data for the oxide perovskite systems; many of which are currently being studied.

#### ACKNOWLEDGMENTS

The authors express their appreciation to Dr. A. Goldmann for use of the SrTiO<sub>3</sub> data, to Dr. M. Campagna for use of the Na<sub>0.8</sub>WO<sub>3</sub> data, and to Dr. V. Henrich for use of the UPS SrTiO<sub>3</sub> data and for many valuable discussions. Acknowledgment is made to the Donors of the Petroleum Research Fund, administered by the American Chemical Society, for partial support of this research.

\*Permanent address: Department of Physics, University of Missouri-Columbia, Mo. 65201.

†On leave from Middle East Technical University, Ankara, Turkey.

<sup>1</sup>F. L. Battye, H. Höchst, and A. Goldmann, Solid State Commun. 19, 269 (1976).

<sup>2</sup>G. K. Wertheim, L. F. Mattheiss, M. Campagna, and T. P. Pearsall, Phys. Rev. Lett. 32, 997 (1974).

- <sup>3</sup>M. Campagna, G. K. Wertheim, H. R. Shanks, F. Zumburg, and E. Banks, *Phys. Rev. Lett.* **34**, 738 (1975).
- <sup>4</sup>J.-N. Chazalviel, M. Campagna, G. K. Wertheim, and H. R. Shanks, *Phys. Rev. B* **16**, 697 (1977).
- <sup>5</sup>V. E. Henrich, G. Dresselhaus, and H. J. Zeiger, *Bull. Am. Phys. Soc.* **22**, 364 (1977); MIT Lincoln Laboratory, Solid State Research Report No. 2, 1976 (unpublished), p. 39.
- <sup>6</sup>S. P. Kowalczyk, F. R. McFeely, L. Ley, V. T. Grimsyn, and D. A. Shirley, *Solid State Commun.* **23**, 161 (1977).
- <sup>7</sup>A. M. Bradshaw *et al.*, *Phys. Rev. B* **16**, 1480 (1977), and references therein.
- <sup>8</sup>L. Kopp, B. N. Harmon, and S. H. Liu, *Solid State Commun.* **22**, 677 (1977).
- <sup>9</sup>S. Ellialtıođlu and T. Wolfram, *Phys. Rev. B* **15**, 5909 (1977). Note, in Eq. (2) of Ref. 9 the factor  $(\overline{p}d\pi)^2$  should be replaced by  $2(pd\pi)^2$  and  $\Delta_p$  should be replaced by  $-\Delta_p$  throughout.
- <sup>10</sup>L. F. Mattheiss, *Phys. Rev. B* **6**, 4718 (1972).
- <sup>11</sup>T. Wolfram, *Phys. Rev. Lett.* **29**, 1383 (1972), T. Wolfram, E. A. Kraut, and F. J. Morin, *Phys. Rev. B* **7**, 1677 (1973).
- <sup>12</sup>M. Cardona, *Phys. Rev.* **140**, A651 (1965).